DESIGN STUDIES OF MAGNET SYSTEMS FOR MUON HELICAL COOLING CHANNELS*

V.V. Kashikhin, V.S. Kashikhin, M. Lamm, M.L. Lopes, A.V. Zlobin#, FNAL, Batavia, IL 60510
M. Alsharo'a, R.P. Johnson, S.A. Kahn, Muons Inc, Batavia, IL 60510, U.S.A.

Abstract

Helical cooling channels with superimposed solenoid and helical dipole and quadrupole coils, and a pressurized gas absorber in the aperture offer high efficiency of 6D muon beam cooling. In this paper, we continue design studies and comparison of two basic concepts of magnet system proposed for a helical cooling channel focusing on the high field sections. The results of magnetic analysis and Lorentz force calculations as well as the superconductor choice are presented and discussed.

INTRODUCTION

Helical cooling channels consisting of a magnet system with superimposed solenoid and helical dipole and quadrupole fields, and a pressurized gas absorber in the aperture offer high efficiency of 6D muon beam cooling for a future Muon Collider and some other applications [1]-[3]. To achieve the required muon beam phase space reduction of the order of 10^5-10^6, the cooling channel is divided into several segments. Each segment has a smaller aperture and stronger fields, to reduce the equilibrium emittance and allow continuous beam cooling.

Two alternative designs of magnet system for the helical cooling channel were proposed and are being investigated at the present time [4]-[5]. The first one is based on a straight large aperture solenoid with helical dipole and quadrupole coils on top of it. The other one consists of a helical solenoid assembled from a number of ring coils and shifted in the transverse direction such that the coil centers form the required equilibrium helical orbit. This structure generates the main solenoidal field and the helical dipole and "quadrupole" (field gradient) components. Both concepts have been developed and compared for the MANX experiment [6].

In this paper, we continue design studies and comparison of two basic concepts of magnet system for a helical cooling channel focusing on the high field sections. The results of magnetic analysis and the considerations on superconductor choice for different sections are presented and discussed.

DESIGN COMPARISON

Conceptual designs of muon HCC, number of sections, their geometrical parameters and field components relevant for a future muon collider, still need to be optimized. Optimization includes accommodation of RF cavities, elements of coil support system and cryostat, service equipment inside the magnet aperture, etc., and providing the required beam cooling.

The main goal of this study was to understand the possibilities and limitations of generating the required field components in high-field sections with given geometrical parameters. To study and compare different magnet designs for multistage HCC, as target parameters we used those reported in [3]. They are summarized in Table 1. Field components in the table are defined in a cylindrical coordinate system (r,τ,z).

Table 1: Target parameters of magnet system for multi-section HCC.

Parameter	Section			
	1st	2nd	3rd	4th
Total length, m	50	40	30	40
Period, m	1.00	0.80	0.60	0.40
Orbit radius, m	0.160	0.130	0.095	0.060
Solenoidal field (B_z), T	-6.95	-8.69	-11.6	-17.3
Helical dipole field (B_τ), T	1.62	2.03	2.71	4.06
Field gradient (dB_τ/dr), T/m	-0.70	-1.10	-2.00	-4.50

Large Bore Straight Solenoid with Helical Coils

Parameters of low-field sections in Table 1 are compatible with the MANX magnet parameters. It was already shown [4] that they could be based on either of the two concepts of helical magnet system. In this subsection, we describe the large bore design and parameters for the highest field HCC section in Table 1.

The 3D magnet model is shown in Fig. 1. It consists of the helical dipole coil placed inside of the straight solenoid. Such configuration was chosen due to the large peak field in the dipole coil.

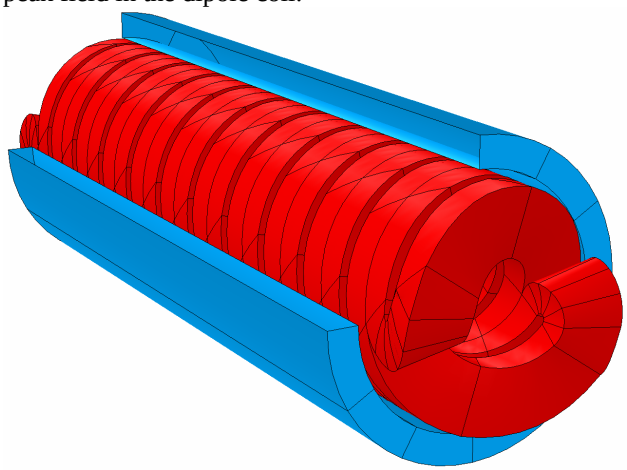

Figure 1: High-field helical dipole with straight solenoid (a quarter removed for clarity).

*This work was supported by the U.S. Department of Energy under SBIR Contract No. DE-FG02-07ER84825.
#zlobin@fnal.gov

The flux density distribution calculated for each coil at the nominal current shows that, although the helical dipole and solenoid need to produce only 4.06 T and 17.3 T respectively, the peak fields in these coils are 34.5 T and 27.5 T respectively.

The required solenoidal and dipole field components were precisely reproduced in this configuration. However, the field gradient of 16 T/m generated by the helical dipole coil is off by an order of magnitude. A dedicated quadrupole coil of a reasonable thickness could correct up to 10% of this value that would still leave a larger than necessary gradient.

The large difference between the field required on the beam orbit and the peak field in the coils is due to the high field gradient across the aperture. As a result, the peak field occurs at the opposite side of the aperture from the beam. Thus, it essentially doubles the coil peak field with respect to the maximum field on the beam orbit.

To achieve the above fields, the high temperature superconductors (HTS) - either the Bi-2223 tape or Bi-2212 round strand, that have similar engineering critical current densities, could be used. Nevertheless, the helical dipole coil has virtually no margin at the operating field, and the solenoid has a small 10% margin. Further increase of the coil thickness in order to gain the extra margin is very inefficient in coils with the thickness comparable to their aperture. Therefore, the operation field in this design with ~50 % margin is limited to 9-10 T, which is well below the required field level in that section.

Helical Solenoid

Helical solenoids were developed for all the four sections in Table 1. For each section, the geometrical parameters were optimized in order to match solenoidal field (primary target) as well as the helical dipole and gradient with some constrains related to magnet period and orbit radius. Five-meter long modules of helical solenoids for the 1st and 4th HCC sections are shown in Fig. 2 and 3.

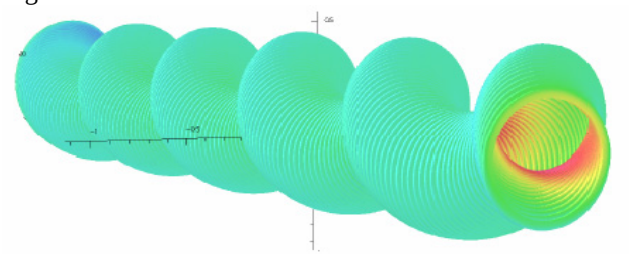

Figure 2: Helical solenoids for low-field section.

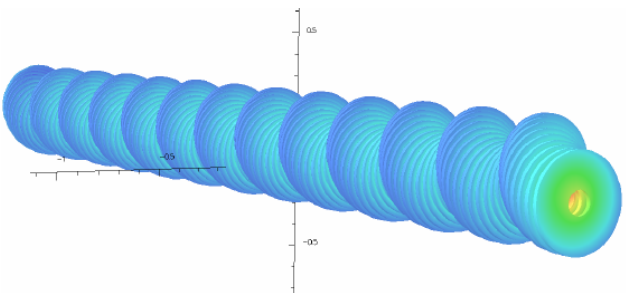

Figure 3: Helical solenoids for high-field section.

Table 2 summarizes the parameters of the helical solenoids for all the four sections. It was not possible to match the helical dipole and quadrupole components simultaneously. Therefore, the values presented in Table 2 are the optimum ones.

Table 2: Helical Solenoid Parameters

Parameter	Section			
	1st	2nd	3rd	4th
Superconductor	Nb_3Sn	Nb_3Sn	Nb_3Sn	BSCCO
Coil ID, mm	460	300	200	100
Coil width, mm	20	16	12	8
Coil radial thickness, mm	50	110	150	150
Solenoidal field, T	-6.95	-8.69	-11.60	-17.30
Helical dipole field, T	1.54	1.95	2.20	2.88
Helical field gradient, T/m	-1.07	-1.84	-2.04	-4.05
Coil maximum field, T	9.53	11.10	13.94	19.54
Current density, A/mm^2	453.1	258.4	244.4	118.1
Safety margin, %	83	70	40	84

The coil width was gradually reduced from section to section to keep the same number of coils per period. Since the critical current density in superconductors reduces with magnetic field, the coil radial thickness increases in higher field sections to provide the required operation field components with some safety margin. In the last two high-field sections, it is comparable with the coil aperture. The safety margin decreases in Nb_3Sn coil with the increase of operation field.

Fig. 4 shows the critical coil current density for Nb_3Sn and HTS coils, coil load lines and operation points for the four sections of HCC. The superconductor properties for Nb_3Sn sections are parameterized using [7] with J_c(12T, 4.2K) = 3 kA/mm^2 and coil packing factor of 0.38. The superconductor properties and coil packing factor for HTS sections are the same as in [8]. The level of maximum field in the three first sections suggests that they could be made of Nb_3Sn superconductor. The fourth section needs HTS.

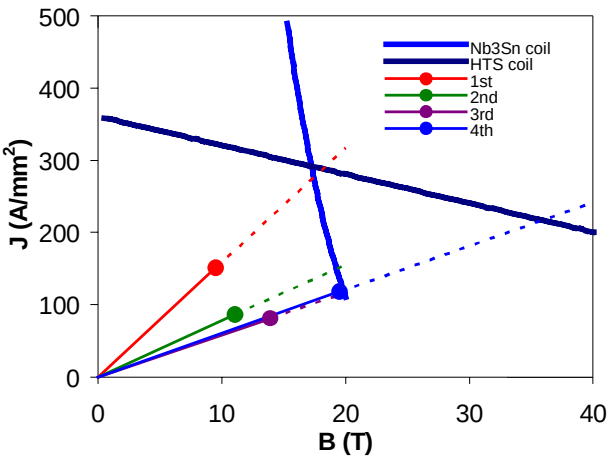

Figure 4: Critical coil current density and load lines for the 1st, 2nd, 3rd and 4th sections.

FIELD CORRECTION

Analysis shows that it is difficult to match simultaneously the solenoidal field and the two transverse field components for the given geometrical parameters. To better understand the adjustability of helical dipole and field gradient in helical solenoids, the sensitivity analysis was performed. Table 3 presents the relative changes of the dipole ($\Delta B/B_0$) and gradient ($\Delta G/G_0$) components due to relative changes of one of the geometrical parameters – helical period ($\Delta\lambda/\lambda_0$), coil inner radius ($\Delta R/R_0$), or coil radial thickness ($\Delta w/w_0$), with respect to their nominal values B_0, G_0, λ_0, R_0 and w_0 (shown in Table 2) for the first and forth sections. The solenoidal field was always kept constant. In all the cases but one, the relative increase of geometrical parameters reduces the helical dipole and field gradient. As can be seen, the helical field gradient is factor of 3 to 15 more sensitive to the variations of the geometrical parameters than the helical dipole in both low-field and high-field sections.

Table 3: Relative sensitivity of dipole and gradient components to relative variations of main geometrical parameters.

Section	$\frac{\left(\frac{\Delta B}{B_o}\right)}{\left(\frac{\Delta\lambda}{\lambda_o}\right)}$	$\frac{\left(\frac{\Delta G}{G_o}\right)}{\left(\frac{\Delta\lambda}{\lambda_o}\right)}$	$\frac{\left(\frac{\Delta B}{B_o}\right)}{\left(\frac{\Delta R}{R_o}\right)}$	$\frac{\left(\frac{\Delta G}{G_o}\right)}{\left(\frac{\Delta R}{R_o}\right)}$	$\frac{\left(\frac{\Delta B}{B_o}\right)}{\left(\frac{\Delta w}{w_o}\right)}$	$\frac{\left(\frac{\Delta G}{G_o}\right)}{\left(\frac{\Delta w}{w_o}\right)}$
1st	-0.06	0.91	-1.16	-6.14	-0.09	-0.46
4th	-0.08	-0.27	-0.80	-4.93	-0.75	-2.15

The possibility of adjusting the all three field components in high-field helical solenoid using external straight correction solenoid was also studied. 5-m long module of 4th section with helical solenoid and correction solenoid is shown in Fig. 5. The geometrical parameters of correction solenoid, maximum field in the coil and field components in the aperture of the helical solenoid are reported in Table 4. Helical and correction solenoids produce opposite longitudinal field components of 24 T and 7 T respectively. The total solenoidal and helical dipole fields are as in Table 1 and the transverse field gradient is ~30% more than required. Based on the results shown in Table 3 it can be tuned by increasing the coil inner radius and/or coil thickness.

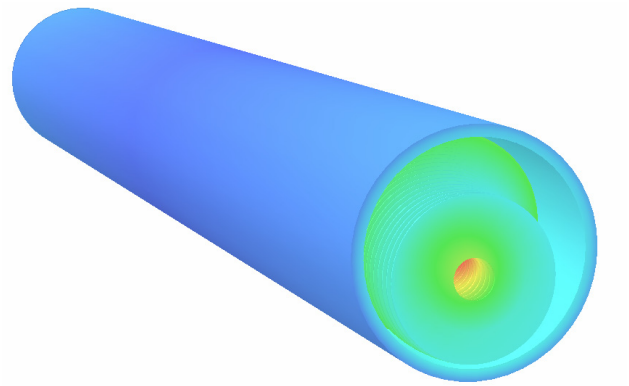

Figure 5: High-field helical solenoid with external correction solenoid.

Table 4: Parameters of high field section of helical cooling channel with helical and correction solenoid.

Parameter	Value
Correction solenoid thickness, mm	30
Correction solenoid ID, mm	540
Operation current density in correction solenoid, A/mm ^{2}	191.3
Solenoidal field, T	-17.3
Helical dipole field, T	4.06
Helical field gradient, T/m	-5.73
Coil maximum field, T	20.46
Nominal helical coil current density, A/mm^2	166.9
Safety margin, %	45

Increasing the coil aperture will provide more room in the aperture for RF and other systems. Increasing the coil thickness will increase the coil operation margin, which reduced in case of correction solenoid from 84 to 45%.

CONCLUSION

Design studies and comparison of two basic concepts of magnet system for a multi-section helical cooling channel show that the design based on a large-aperture straight solenoid is limited by 9-10 T solenoidal fields. The cooling sections with higher fields have to use helical solenoids with Nb_3Sn, HTS or hybrid coils. The different possibilities of achieving the required field components using solenoid geometrical parameters and external correction solenoid were demonstrated.

REFERENCES

[1] Y. Derbenev and R. Johnson, “Six-Dimensional Muon Cooling Using a Homogeneous Absorber”, Phys. Rev. ST AB, 8, 041002 (2005).

[2] K Yonehara et al. “Simulations of a Gas-Filled Helical Muon Beam Cooling Channel”, Proc. of PAC2005, Knoxville, TN, 2005, pp. 3215-3217.

[3] K. Yonehara et al, “Studies of a Gas-Filled Helical Muon Cooling Channel”, Proc. of EPAC2006, Edinburgh, Scotland, pp. 2424-2426.

[4] V.S. Kashikhin et al., “Superconducting Magnet System for Muon Beam Cooling”, IEEE Trans. on Applied Superconductivity, Vol. 17, Issue 2, June 2007, pp.1055-1058.

[5] S.A. Kahn et al., “Magnet System for Helical Muon Cooling Channels”, Proc. of PAC2007, Albuquerque, NM, USA, pp.443-445.

[6] V. Kashikhin et al, “Magnets for the MANX 6-D Muon Cooling Demonstration Experiment”, Proc. of PAC2007, Albuquerque, NM, USA, pp. 461-463.

[7] L.T. Summers et al., “A model for the prediction of Nb_3Sn critical current as a function of field, temperature, strain, and radiation damage,” IEEE Trans. on Magnetics, Vol. 27, Issue 2, March 1991, pp. 2041-2044.

[8] V.V. Kashikhin et al., “Study of High Field Superconducting Solenoids for Muon Beam Cooling”, IEEE Trans. on Applied Superconductivity, Vol. 18, Issue 2, June 2007, pp. 928–932.